Tungsten oxide fiber dissolution and persistence in artificial human lung fluids

Tungsten Oxide Fiber Dissolution and Persistence in Artificial Human Lung Fluids

A B Stefaniak and M Chirila

National Institute for Occupational Safety and Health, Morgantown, WV, USA, 26505

E-mail: AStefaniak@cdc.gov

Abstract. Tungsten is a dense metal that is used in a range of industrial applications, including non-sag wire for light bulb filaments. During the conversion of tungsten oxide powder into tungsten metal powder for use as filaments, aerosols may be generated which contain tungsten sub-oxide particles having fiber morphology. To evaluate whether these fibers pose a yet unrecognized inhalation hazard due in part to their biodurability, we characterized the physicochemical properties and measured relative dissolution of fiber-containing ($WO_{2.81}$, $WO_{2.66}$, $WO_{2.51}$) and isometric-shaped ($WO_{3.00}$, $WO_{2.98}$) powders in artificial lung fluids. Raman spectroscopy results present a shift in the main frequencies for tungsten oxide samples that were sonicated in surfactant, confirming a decrease in the size of the crystalline domains by de-agglomeration. Geometric mean fiber aspect ratios were 8.3 ($WO_{2.81}$), 7.9 ($WO_{2.66}$), and 6.9 ($WO_{2.51}$). In artificial extracellular lung fluid, alkylbenzyldimethylammonium chloride (ABDC), added to prevent mold growth during experiments, inhibited ($p < 0.05$) dissolution of $WO_{2.98}$, $WO_{2.81}$, and $WO_{2.66}$. Less ($p < 0.05$) of the fibrous $WO_{2.66}$ and $WO_{2.51}$ dissolved relative to W metal; however, biodurability was only modestly greater than W metal. These data are useful for understanding the inhalation dosimetry of fibrous and non-fibrous forms of tungsten oxide materials.

1. Introduction

Tungsten is a dense metal that is used in a wide range of applications, including non-sag wire for filaments in light bulbs [1-3]. The manufacture of tungsten for non-sag wire begins with the calcining of ammonium paratungstate to yield tungsten oxide powder, which in turn, is reduced under controlled conditions to yield tungsten metal powder. During the production of tungsten metal powder, aerosols may be generated which contain tungsten sub-oxide particles having fibrous morphology [4-8]. The potential toxicity of tungsten sub-oxide fibers is poorly understood; however, in one preliminary study, these materials generated free radicals [7]. The capacity, if any, of tungsten sub-oxide fibers to contribute to development of adverse pulmonary health effects is currently not well understood.

Results of limited air sampling in occupational environments suggests that tungsten oxide fibers are respirable, with fibers generally having diameter <0.3 μm and very few fibers having length >5 μm [4-8]. Both single fibers and aggregates of fibers have been identified in air samples [4-6]. Fiber dimensions determine the extent to which fibers are inhaled, retained, and cleared by the lung. In humans engaged in mouth breathing, deposition in the alveolar region of the lung is maximal for fibers having aerodynamic diameter of 2 μm and aspect ratios (length/width) in the range 3 to 20 [9]. Biopersistence of inhaled fibers is determined by the rate at which they are physically cleared from the lung by mechanical action and the rate at which they dissolve in the lung (biodurability) [9]. Fibers

with length greater than 20 μm probably cannot be engulfed by a single macrophage and will remain in the lung if durable. Fibers with length between 5 and 20 μm may inhibit lung macrophage mobility (i.e., mechanical clearance) in a graded fashion. Mechanical clearance of fibers <5 μm by lung macrophages is probably not influenced by fiber length [10]. The chemistry of fibers, in part, determines their biodurability via dissolution, which occurs in the extracellular lung fluid and/or within lung macrophage phagolysosomes [9].

We characterized the physicochemical properties of five tungsten oxide materials and began to evaluate the hypothesis that tungsten oxide fibers are more biodurable than isometric-shaped tungsten oxide particles and tungsten metal in lung fluids. Particle solubility was measured in variations of artificial extracellular lung fluid and lung alveolar macrophage phagolysosomal fluid to evaluate solvent effects on observed dissolution rates.

2. Materials and Methods

2.1. Study powders

Five bulk tungsten oxide powders were obtained from an industrial producer for study: $WO_{3.00}$, $WO_{2.98}$, $WO_{2.81}$, $WO_{2.66}$, and $WO_{2.51}$. With the exception of the $WO_{3.00}$ material, the oxidative states of these powders are average values. The $WO_{3.00}$ and $WO_{2.98}$ powders consisted of isometric-shaped particles and accounted for approximately 80% of this manufacturer's production. The $WO_{2.81}$, $WO_{2.66}$, and $WO_{2.51}$ powders contained fiber-shaped particles and accounted for the remaining 20% of industrial production. Physicochemical properties of these five tungsten oxide materials, and for comparison a pure tungsten metal powder, were characterized prior to estimation of biodurability in artificial lung fluids. A static dissolution technique was chosen for the biodurability studies because it has been shown to provide results for beryllium oxide that were nearly identical to in vivo models [11].

2.2. Characterization of study powders

Physical characterization of study materials included scanning electron microscopy (SEM) to evaluate particle morphology and size, helium pycnometry to determine density, and nitrogen gas adsorption to determine specific surface area (SSA). Raman spectroscopy was used to investigate the morphology and aggregation state of tungsten oxide fibers. For these experiments, we compared dry tungsten oxide powders (as received) with samples prepared by mixing the powder with artificial extracellular lung fluid (SUF) at a concentration of 4 mg mL^{-1}. The liquid samples were sonicated for 30 min. For collection of spectra, a small amount of powder was set to a glass fiber filter on a microscope slide. In the case of liquid samples, two silicon wells were firmly attached to a microscope slide and 100 μL of suspension was added to the slide. Raman spectra were collected using a with an excitation wavelength of 514.5 nm. The laser beam was focused through a microscope down to an approximate diameter of 10 μm and the power measured before the microscope was 1 mW. A CCD was used to detect the Raman signal in the region (80 – 1000) cm^{-1} where tungsten oxide exhibits main vibrations frequencies characteristic to both bulk and microcrystalline domains [12,13].

Chemical characterization of study materials included O content and 35 impurities: Ag, Al, As, Ba, Be, C, Ca, Cd, Co, Cr, Cu, Fe, H, K, La, Li, Mg, Mn, Mo, N, Ni, P, Pb, S, Sb, Se, Sn, Sr, Te, Ti, Tl, V, Y, Zn, and Zr. X-ray photoelectron spectroscopy was used to determine surface elemental chemistry (to a depth of approximately 20 Å).

2.3. Artificial lung fluid solubility studies

To estimate solubility, a known mass of each powder was weighed on a 0.025-μm pore size 47-mm diameter mixed cellulose ester filter (Millipore, Bedford, MA) then covered with a second filter. This filter "sandwich" was secured tightly in a static dissolution chamber (Intox Products, Moriarity, NM) using four nylon screws to provide a particle-tight seal around the edge of the sandwich. Each chamber was immersed in 80 mL of SUF or artificial macrophage phagolysosomal simulant fluid

(PSF) in a polypropylene plastic beaker and maintained at 37 °C for the duration of the study. For each dissolution experiment, triplicate samples were prepared for each study powder. At each time point, the chamber was removed from its beaker, the fluid transferred to a borosilicate glass jar, and fresh equilibrated fluid added to the sample beaker. Samples were stored frozen at -5°C and thawed prior to quantification of dissolved W in accordance with U.S. OSHA Method 213 (inductively coupled plasma-atomic emission spectroscopy).

2.3.1. *Artificial extracellular lung fluid.* SUF was prepared as previously described [14]. The pH of SUF was maintained at 7.3±0.1 for the duration of the dissolution experiments by blanketing the headspace in each sample beaker with a 5% CO_2/95% air mixture. The recipe for preparation of SUF includes 50 ppm of ABDC, which is added to prevent mold growth during experiments. ABDC is not a constituent of human extracellular lung fluid. To determine whether the presence of this exogenous constituent artificially influenced dissolution, dissolution of each study powder was measured using SUF prepared with and without ABDC; solvent was changed at 1, 4, 24, and 72 hours.

2.3.2. *Artificial macrophage phagolysosomal fluid.* To simulate the acidic conditions encountered by particles that are phagocytised by lung alveolar macrophages, PSF was prepared as described by Stefaniak et al. [15]. The pH of the PSF solution was maintained at 4.55±0.10 for the duration of the dissolution experiments. As with SUF, a preliminary experiment was performed using each study powder to evaluate whether ABDC artificially influenced dissolution. Our *a priori* assumption was that material dissolution would be faster in the more acidic PSF solvent relative to the neutral pH of the SUF solvent. As such, solvent in each sample beaker was changed at 1, 4, 8, 24, 48, and 72 hours to evaluate whether dissolution behaviour was linear or multiphasic under acidic conditions.

3. Results and Discussion

3.1. Characteristics of study powders

Table 1 summarizes the physical properties of the five study powders. As expected, density generally increased as powder oxygen content decreased. SSA varied by a factor of 15 among powders. Figure 1 illustrates the morphology of the dry tungsten oxide study powders. $WO_{3.00}$ and $WO_{2.98}$ were large (*ca.* 30 μm) compact cube-shaped particles, some with rounded edges, whereas $WO_{2.81}$, $WO_{2.66}$, and $WO_{2.51}$ were mixtures of fibers and compact cube-shaped particles. Tungsten metal was aggregate clusters of 1.2 μm primary particles. Among all fiber-containing materials, geometric mean (GM) fiber lengths were ≤ 5 μm and diameters ranged from 0.5 to 0.6 μm. GM fiber aspect ratios (length/width) determined from SEM images decreased as powder oxygen content decreased. The GM aerodynamic fiber diameter, calculated from the equation of Cox [16] assuming motion perpendicular to the fiber's axis, was 2.3, 3.1, and 2.1 μm for $WO_{2.81}$, $WO_{2.66}$, and $WO_{2.51}$, respectively. Fibers with these aerodynamic sizes and aspect ratios have high probability of depositing in the non-ciliated alveolar region of the lung [9]. The dimensions of fibers in these bulk tungsten oxide powders are consistent with previous reports that airborne tungsten oxide fibers were generally respirable, with most fibers having diameter <0.3 μm and very few fibers having length >5 μm [4-8]. Additionally, the SEM images illustrate both single and aggregated fiber, consistent with morphologies observed for airborne tungsten oxide fibers in workplace air.

Figure 2 presents the Raman spectra of the tungsten oxide study materials. No major differences were observed between spectra when tungsten oxide powder was suspended in SUF with or without ABDC (data not shown). The WO_3, $WO_{2.98}$, and $WO_{2.81}$ powders displayed intense bands around 718 and 807 cm^{-1} which are characteristic to stretching mode of ν(O – W – O) [12]. As the concentration of oxygen decreased these two bands decreased as shown for the $WO_{2.66}$ and $WO_{2.51}$ powders [17]. Other important Raman bands observed from our samples include the in-plane bending modes δ(O – W – O) with frequencies at 275 and 325 cm^{-1} and lattice modes at 94 cm^{-1} and 136 cm^{-1}, respectively.

Relative to the main Raman frequencies observed for the dry tungsten oxide powders, when these materials were suspended in SUF most of the bands were observed to shift to lower frequencies. Additionally, a new lattice mode at 94 cm^{-1} becomes noticeable. These results can be interpreted as a decrease in size of the microcrystalline domain from about 100 nm to 35 nm [13] after the tungsten oxide was sonicated in SUF. Note that when we mixed the tungsten oxide powders with phosphate buffered saline solution, no shift or new bands were observed. The time and power of the ultrasonic treatment was not believed to be sufficient to break or damage the particles. As such, the decrease in the microcrystalline domain was interpreted to be the result of de-aggregation of larger particles.

Table 1. Physical properties of tungsten oxide and metal powder study materials.

				GM (GSD)		
Study Material	Formula	Density ($g\ cm^{-3}$)	SSA ($m^2\ g^{-1}$)	L (µm)	W (µm)	AR
"Yellow" tungsten oxide	WO_3	7.2±0.01	0.75±0.03	NA[a]	31.1 (1.8)	NA
TB "Blue" tungsten oxide	$WO_{2.98}$	7.0±0.02	11.10±0.76	NA	29.8 (2.0)	NA
"Blue" high tungsten oxide	$WO_{2.81}$	7.1±0.00	2.85±0.02	4.0 (1.9)	0.5 (1.5)	8.3 (1.8)
"Blue" tungsten oxide	$WO_{2.66}$	8.2±0.03	1.50±0.07	4.9 (1.5)	0.6 (1.4)	7.9 (1.7)
"Blue" low tungsten oxide	$WO_{2.51}$	7.7±0.05	2.10±0.02	3.1 (1.7)	0.5 (1.4)	6.9 (1.8)
Tungsten metal	W	19.6±0.30	0.68±0.09	NA	1.2 (1.4)[b]	NA

[a] NA = Not applicable for isometric-shaped particles
[b] Primary particle size

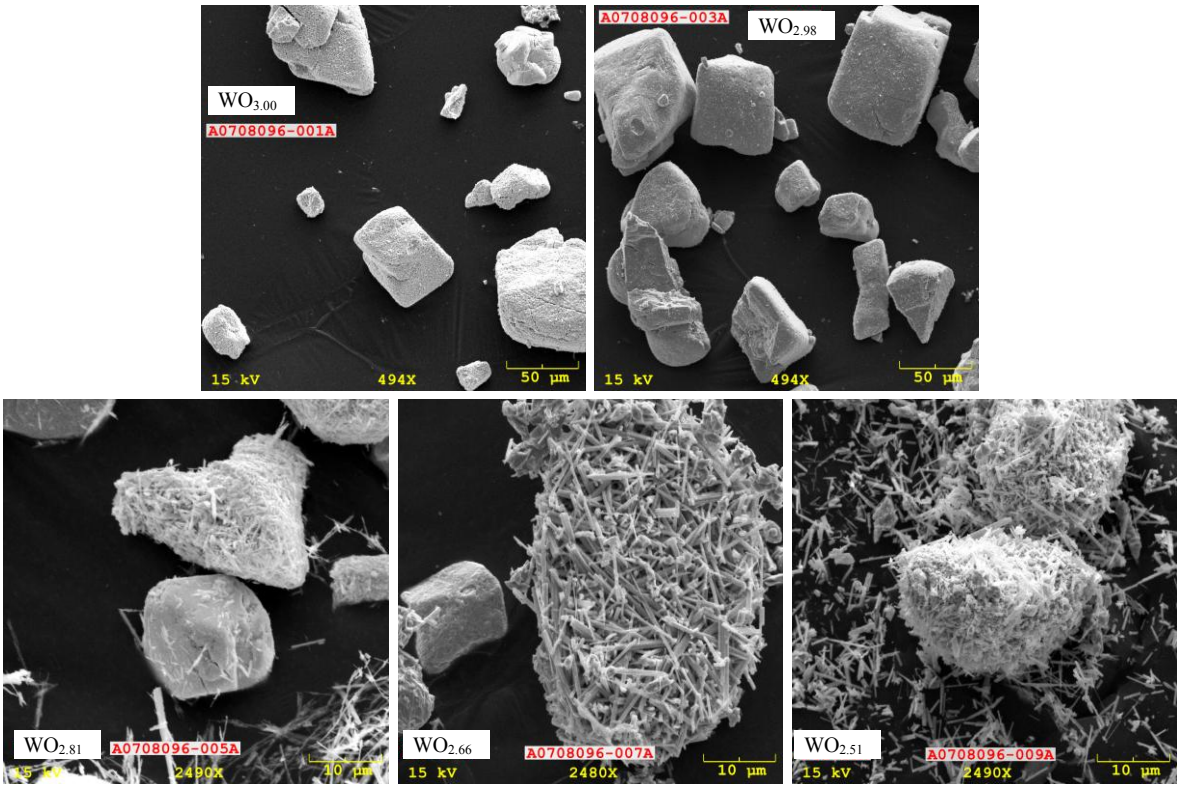

Figure 1. Scanning electron micrographs of tungsten oxide materials illustrating particle morphologies.

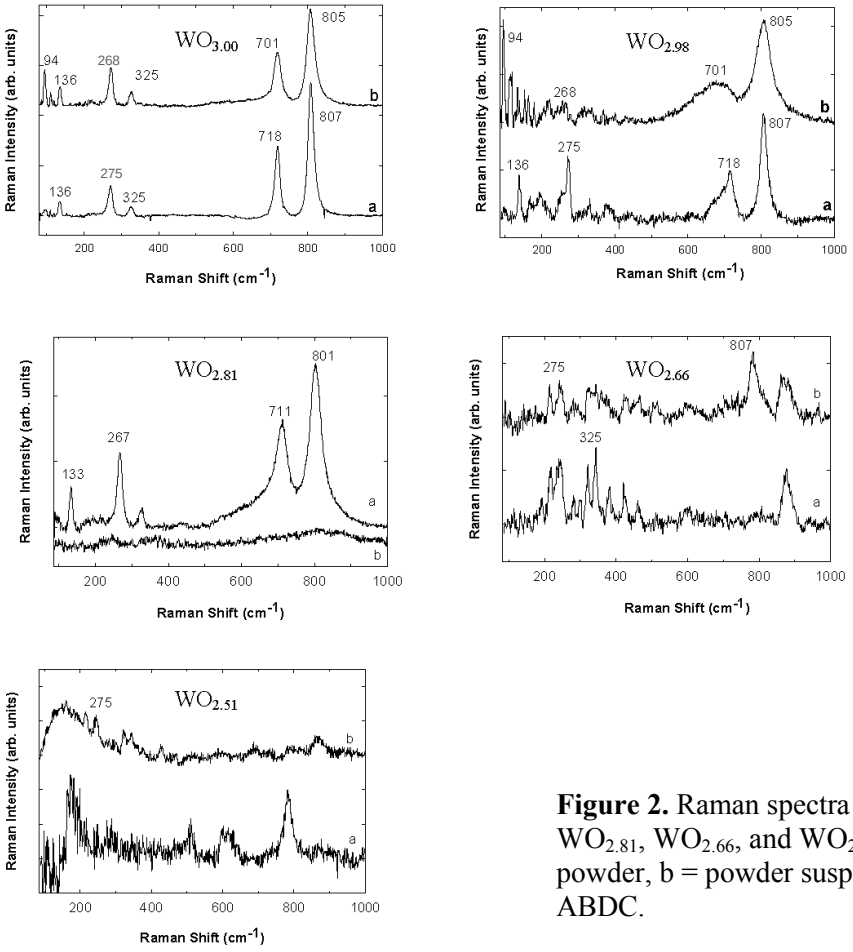

Figure 2. Raman spectra from $WO_{3.00}$, $WO_{2.98}$, $WO_{2.81}$, $WO_{2.66}$, and $WO_{2.51}$ powders. a = dry powder, b = powder suspended in SUF with ABDC.

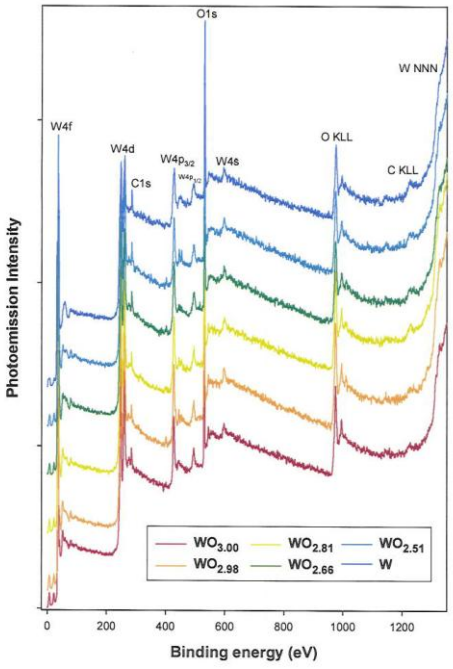

Figure 3. X-ray photoelectron spectroscopy survey spectra of tungsten oxide materials and tungsten metal for comparison. Surfaces of the tungsten oxide and tungsten metal powders were W, O, and minor amounts of C.

As illustrated in figure 3, tungsten oxide powder surfaces were composed of W, O, and minor amounts of C which was consistent with tungsten oxide. Levels of impurities were all ≤ 0.001% by weight in all powders. Thus, the study powders were high purity tungsten oxide materials.

3.2. Artificial lung fluid solubility studies

Figure 4 is a plot of the mass fraction of tungsten dissolved from each of the five bulk tungsten oxide materials in SUF. At the time of this writing, quantification of dissolved tungsten from bulk tungsten oxide materials exposed to PSF was in progress; therefore, only results from studies with SUF are reported herein. A t-test of sample means indicated that, in SUF, ABDC inhibited ($p < 0.05$) dissolution of $WO_{2.98}$, $WO_{2.81}$, and $WO_{2.66}$ but not $WO_{3.00}$ or $WO_{2.51}$. The exact mechanism by which ABDC inhibited dissolution of certain tungsten oxide materials is unknown; however, this anti-fungal agent is a cationic surfactant which may chemically interact with powder surfaces to inhibit dissolution. There was no statistical difference in dissolution between the isometric-shaped $WO_{3.00}$ and tungsten metal particles. The fibrous $WO_{2.66}$ and $WO_{2.51}$ materials dissolved more slowly ($p < 0.05$) than the isometric tungsten metal particles, indicating potential for prolonged biodurability of these fiber materials in human extracellular lung fluid due to the unique chemistry. Note that the biological relevance of this observed difference in dissolution rates has yet to be elucidated. Biopersistence of inhaled fibers is determined by the rate at which they are mechanically cleared from the lung and their biodurability, which is influenced by fiber chemistry [9] and the biological fluid to which the fiber is exposed. As such, fiber biodurability via dissolution may differ between the neutral pH extracellular lung fluid and the acidic fluid encountered upon engulfment by lung macrophage cells and sequestration in phagolysosomes.

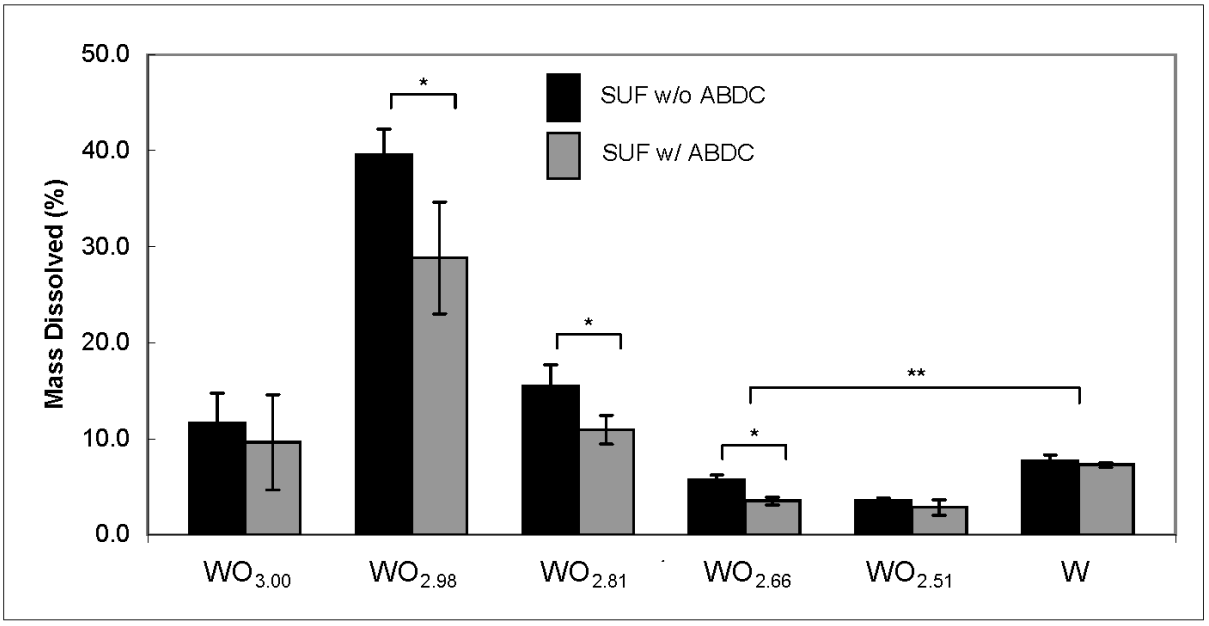

Figure 4. Total mass fraction of tungsten dissolved in 72 hours from various bulk tungsten oxide powders using serum ultrafiltrate (SUF) without and with alkylbenzyldimethylammonium chloride (ABDC), which is added to prevent mold growth during experiments. For comparison, the mass fraction of tungsten dissolved from bulk tungsten metal (W) powder in SUF without and with ABDC is included in the plot. * = difference in dissolution for SUF without and with ABDC ($p < 0.05$ using two-sided t-test assuming equal variances). ** = dissolution in SUF without ABDC lower than tungsten metal ($p < 0.05$ using one-sided t-test assuming equal variances).

4. Summary

Five tungsten oxide powder materials were characterized and their dissolution behavior evaluated in SUF relative to pure W metal. Powder physicochemical properties were unique among study materials. Additionally, Raman spectroscopy was shown to be useful for determination of the morphology and crystalline domain of tungsten oxides. On a mass basis, the rank order of tungsten dissolution (from greatest to least) was: $WO_{2.98} > WO_{2.81} > WO_{3.00} > W > WO_{2.66} > WO_{2.51}$. Fibrous $WO_{2.66}$ and $WO_{2.51}$ materials are potentially more biodurable than isometric shaped tungsten oxide and tungsten metal powders; however, all three materials are poorly soluble. Knowledge gained from these dissolution studies will aid in determining whether the biodurability of these tungsten oxide fiber materials contribute a potential hazard due to prolonged biopersistence in the lung.

Acknowledgements

This research was supported in part by the National Toxicology Program through Interagency Agreement number Y1-ES-9045-10 with the National Institute for Occupational Safety and Health. Mention of a specific product or company does not constitute endorsement by the Centers for Disease Control and Prevention. The findings and conclusions in this report are those of the authors and do not necessarily represent the views of the National Institute for Occupational Safety and Health.

References

[1] Lassner E and Schubert W-D 1995 *Int. J. Refract. Metals Hard Mat.* **13** 111-17
[2] Lunk H-J, Ziemer B, Salmen M, and Heidemann D 1993-1994 *Refract. Metals Hard Mat.* **12** 17-26
[3] Bartha L, Kiss AB, and Szalay T 1995 *Int. J. Refract. Metals Hard Mat.* **13** 77-91
[4] Sahle W 1992 *Chest* **102** 1310
[5] Sahle W, Laszlo I, Krantz S, and Christensson B 1994 *Ann. Occup. Hyg.* **38** 37-44
[6] Sahle W, Krantz S, Christensson B, and Laszlo I 1996 *Sci. Total Environ.* **191** 153-67
[7] Leanderson P and Sahle W 1995 *Toxicol. In Vitro.* **9** 175-83
[8] McKernan JL, Toraason MA, Fernback JE 2008 *J Occup Environ Hyg*. **5** 463-474
[9] Oberdörster G 2002 *Inhal. Toxicol.* **14** 29-56
[10] Davis JMG 1994 *Environ. Health Perspect.* **102(Suppl 5)** 113-17
[11] Stefaniak AB, Day GA, Hoover MD, Breysse PN, Scripsick RC 2006 *Toxicol. In Vitro.* **20** 82-95
[12] Ingham B, Chong SV, and Tallon JL 2005 *J. Phys. Chem. B* **109** 4936-40
[13] Boulova M, Lucazeau G 2002 *J. Solid State Chem*. **167** 425-34
[14] Finch GL, Mewhinney JA, Eidson AF, Hoover MD, and Rothenberg SJ 1988 *J. Aerosol Sci.* **19** 333-42
[15] Stefaniak AB, Guilmette RA, Day GA, Hoover MD, Breysse PN, and Scripsick RC 2005 *Toxicol. In Vitro.* **19** 123-34
[16] Cox RG 1970 *J. Fluid Mech.* **44** 791-810
[17] Wang XP, Yang BQ, Zhang HX, Feng PX 2007 *Nanoscale Res. Lett*. **2** 405-09